scientific reports

Check for updates

OPEN

Schisandrin B alleviates testicular inflammation and Sertoli cell apoptosis via AR-JNK pathway

Bo-Yang Zhang[1,3], Rui Yang[1,3], Wen-Qian Zhu[1], Chun-Ling Zhu[1,2], Lan-Xin Chen[1], Yan-Sen Zhao[1], Yan Zhang[1], Yue-Qi Wang[1], Dao-Zhen Jiang[1], Bo Tang[1] & Xue-Ming Zhang[1]✉

Bacterial testicular inflammation is one of the important causes of male infertility. Using plant-derived compounds to overcome the side effects of antibiotics is an alternative treatment strategy for many diseases. Schizandrin B (SchB) is a bioactive compound of herbal medicine *Schisandra chinensis* which has multiple pharmacological effects. However its effect and the mechanism against testicular inflammation are unknown. Here we tackled these questions using models of lipopolysaccharide (LPS)-induced mice and -Sertoli cells (SCs). Histologically, SchB ameliorated the LPS-induced damages of the seminiferous epithelium and blood-testicular barrier, and reduced the production of pro-inflammatory mediators in mouse testes. Furthermore, SchB decreased the levels of pro-inflammatory mediators and inhibited the nuclear factor kB (NF-κB) and MAPK (especially JNK) signaling pathway phosphorylation in LPS-induced mSCs. The bioinformatics analysis based on receptor prediction and the molecular docking was further conducted. We targeted androgen receptor (AR) and illustrated that AR might bind with SchB in its function. Further experiments indicate that the AR expression was upregulated by LPS stimulation, while SchB treatment reversed this phenomenon; similarly, the expression of the JNK-related proteins and apoptotic-related protein were also reversed after AR activator treatment. Together, SchB mitigates LPS-induced inflammation and apoptosis by inhibiting the AR-JNK pathway.

Keywords Apoptosis, Inflammation, Mouse, Testicular inflammation, Schizandrin B, Sertoli cell

In recent years, infertility has become a serious male health problem. The sperm densities in men have fallen by 52.4% and sperm counts by about 60% over the past four decades[1]. Inflammation in male reproductive system caused by infections are important factors of male infertility, among which testicular inflammation often leads to male infertility[2]. Testicular inflammation is usually characterized by inflammatory cell infiltration and damage to the seminiferous tubules, especially the blood-testicular barrier (BTB)[3,4]. Therefore, how to ameliorate testicular inflammation is of great importance. Currently, the therapy of testicular inflammation mainly relies on antibiotics; however, its side effects are inevitable.

To overcome the side effects of antibiotics, using plant-derived bioactive compounds might provide solutions. Schisandra chinensis (Turcz.) Baill. (*S. chinensis*) is a plant well-known in traditional Chinese medicine and also in herbal medicine of other East Asia countries[5]. The versatile effects of its fruits on the gastrointestinal system, respiratory system, cardiovascular system, central nervous system, and male reproductive system, have been recorded[6–8]. However, its main effective components specific to testicular diseases as well the underlying mechanisms are still unclear. *S. chinensis* fruits contain many Schisandra lignans with strong pharmacological activities. Schisandrin B (SchB) is one of them[9], which has functions of protecting liver, anti-oxidation, anti-tumor, and preventing neurodegenerative diseases[9–12]. SchB also benefits the adult neurogenesis[13–16], and can improve renal function of IgA Nephropathy Rats[17]. However, whether it prevents or alleviates testicular inflammation is unknown. Addressing this question might partly explain its ancient pharmacological activity on male reproduction at molecular lever.

[1]State Key Laboratory for Diagnosis and Treatment of Severe Zoonotic Infectious Diseases, Key Laboratory for Zoonosis Research of the Ministry of Education, College of Veterinary Medicine, Jilin University, Changchun, China. [2]College of Animal Science and Veterinary Medicine, Henan Institute of Science and Technology, Xinxiang 453003, China. [3]These authors contributed equally: Bo-Yang Zhang and Rui Yang. ✉email: zhangxuem@jlu.edu.cn

Here we hypothesize that SchB can mitigate testicular inflammation. To test this hypothesis and reveal the underlying mechanism, lipopolysaccharide (LPS), a regular reagent for preparation of inflammatory model, was used to induce mouse testicular inflammation as the in vivo model, and LPS-induced mouse Sertoli cells (mSCs) was employed as the in vitro model because SCs are the most important somatic cells and play pivotal roles in maintaining spermatogenic niche/microenvironment, particularly the BTB. The SCs have several essential functions such as support, nutrition, release, secretion, immune immunity, and phagocytosis in spermatogenesis[18]. As the main structure of the BTB, SCs secrete immunoregulatory factors such as interleukin-1 (IL-1), IL-6, tumor necrosis factor-α (TNF-α), transforming growth factor-β (TGF-β), cyclooxygenase 2 (COX-2), and induced nitric oxidesynthase (iNOS) to form a cytokine network and regulate the local immune function. They also generate androgen-binding protein which binds androgen receptor (AR) to keep a high androgen concentration in the seminiferous epithelium[19]. By contrast, testicular inflammation usually destroys spermatogenic niche, resulting in the impairment, apoptosis and especially tight junction (e.g. Claudin-1 and ZO-1) destruction of SCs[2]. Therefore, the LPS-stimulated SCs can serve as an excellent in vitro model for testicular inflammation.

Materials and methods

Materials

SchB (purity ≥ 98%) and LPS from Escherichia coli O55:B5 were bought from Shanghai Yuan Ye Bio-technology (Shanghai, China). The primary antibodies against phospho-NF-κB p65 (#3033) and phospho-p38 (#4511) were provided by Cell Signaling Technology (Beverly, MA, USA). Antibodies against COX-2 (12,375–1-AP), iNOS (18,985–1-AP), NF-κB p65 (66,535–1-lg), p38 (66,234–1-lg), ERK1/2 (67,170–1-ig), JNK1/2 (66,210–1-lg), Claudin 1 (13,050–1-AP), ZO-1 (21,773–1-AP) and β-actin (66,009–1-lg) were purchased from Proteintech (Wuhan, China). Antibodies for phospho-ERK1/2 (BM5446) and phospho-JNK1/2 (BM4383) were supplied by BOSTER (Wuhan, China). Caspase 3 (R23727), Bax (R22708) and Bcl2 (381,702) were acquired from ZEN Bio (Chengdu, China). The culture medium and ingredients were sourced from (Procell, Wuhan, China).

Testicular inflammation model

C57BL/6 (7–8 weeks old) male mice were provided by the Experimental Animal Center of Bethune Medical College of Jilin University. They were caged at 22 -23 °C, 12 h light and dark cycle, and ad libitum access to food and water. The whole study is approved by the development of Animal Care and Use Committee of Jilin University, and all animal care and experimental procedures are under the supervision of this committee. Furthermore, the experiment was carried out in compliance with the revised ARRIVE guidelines 2.0. SchB was dissolved in olive oil (O815211, MACKLIN, Shanghai, China) and two concentrations (40 and 80 mg/kg/day) were selected for the following treatments based on our preliminary experiments. Mouse testicular inflammation was established as previously described with minor modifications[4]. The animals were randomly assigned to 6 groups with 6 animals in each group, the control (Con), olive oil control (Oil), 80 mg/kg/day SchB treated group (SchB80), 10 mg/kg LPS-induced testicular inflammation (LPS), 40 mg/kg/day SchB + 10 mg/kg LPS ($SchB_{40}$LPS), and 80 mg/kg/day SchB + 10 mg/kg LPS ($SchB_{80}$LPS). Before LPS intraperitoneal injection, oral SchB administration was medicated intragastrically for consecutive three days. At 12 h after LPS injection, the mice were euthanized by cervical dislocation under deep anesthesia by isoflurane, and the testes were collected for the follow-up experiments.

Histopathological examination

The testicular tissues were embedded in paraffin wax after fixation in 4% formaldehyde solution for 24 h to create 5 μm-thick slices. In order to observe the histopathological changes of the testicular tissues, the sections were stained with hematoxylin–eosin (HE) regularly, observed and photographed under a light microscope.

Immunofluorescence assay

The paraffin sections were used for immunofluorescent staining. Briefly, the sections were deparaffinized, rehydrated, and further subjected to ethylene diamine tetraacetic acid (EDTA) antigen retrieval buffer (pH 8.0). Then the sections were blocked with 3% bovine serum albumin (w/v) for 30 min. Subsequently, they were incubated overnight at 4 °C with rabbit anti-Claudin-1 and rabbit anti-ZO-1 (both 1:1000, respectively). Next, the sections were incubated with Alexa Fluor 488-conjugated goat anti-rabbit IgG (S0018, 1:200, Affinity Biosciences, Jiangsu, China) for 60 min. To visualize the nuclei, the samples were counterstained with 4', 6-diamidino-2-phenylindole (DAPI, Beyotim Biotechnology, Shanghai, China) and incubated at room temperature for 15 min. Finally, the sections were covered with anti-quenching tablets and observed under a Nikon 80i fluorescence microscope. The sections stained with isotype IgG served as the negative control. For the fluorescence intensity analysis, at least three visual fields were selected randomly in each group.

Cell culture and treatment

The mSCs (Procell CL-0456, TM4) and human macrophage cell line THP-1 (CL-0233) were provided by Procell Life Science & Technology Co., Ltd, cultured in DMEM/F12 (PM150312) with 5% Hartmann's solution (164,215–500), 2.5% fetal bovine serum (FBS, 164,210–500), and 1% penicillin–streptomycin (PB180120), in a 37 °C incubator with 5% CO_2. When mSCs were cultured to 80–90% confluence, they were collected and seeded into 6-well plates or 96-well plates. When the cell confluence reaches 70%, they were pretreated with 5 μM SchB (determined by CCK8 analysis) for 2 h and stimulated with 1 μg/ml LPS for 12 h according to our previous work[4], and then collected for subsequent experiments.

Cell viability analysis

The Cell Counting Kit-8 (CCK-8, Saint-Bio, Shanghai, China) was applied to test whether SchB affects the cell viability. The mSCs were cultured in a 96-well plate for 12 h. After cultured 3 h in serum-free medium, the cells were treated with SchB at different molar concentrations (5, 10, 15, 20, 30 and 40 μM) for 2 h, followed by exposure to -/LPS (1 μg/ml) for 12 h. Subsequently, the cells in each well were incubated for 1 h after adding 10 μl CCK-8 solution. Finally, the absorbance at 450 nm was recorded.

Western blot

To obtain the total protein, mouse testicular tissues and the mSCs were lysed with lysis buffer (Beyotime, Shanghai, China), followed by centrifugation for 15 min at 12,000 g. The supernatants containing the total protein were collected. Subsequently, the protein concentrations were determined by using the BCA Protein Assay Kit (ThermoFisher Scientific, Waltham, MA, USA) according to the manufacturer's instructions. Protein samples were loaded onto 6–15% SDS-PAGE at 110 V for 90 min and then transferred onto a polyvinylidene difluoride membrane (Millipore, Darmstadt, Germany) at 75 V for 1 h. The transferred membranes were blocked in 0.1% Tris buffered saline-Tween (TBS-T) containing 5% skim milk for 2 h, followed by incubation overnight at 4 °C with each primary antibody in TBS-T containing 5% bovine serum albumin (Gentihold, Beijing, China). After washing 5 times with TBS-T, the membranes were co-incubated with the corresponding horseradish peroxidase-labeled secondary antibodies (1:3000, Bosterbio, USA) at room temperature for 1 h. Finally, the immunoreactive blots were visualized with an enhanced chemiluminescent substrate (ThermoFisher Scientific, Waltham, MA, USA).

Quantitative real-time reverse transcription-PCR (qRT-PCR)

Total RNAs were isolated from three testes in each group or the mSCs by using the TRIZOL reagent (Invitrogen, Carlsbad, CA, USA) and then reverse-transcripted into cDNAs by using the Revert Aid First Strand cDNA Synthesis Kit (ThermoFisher Scientific, Waltham, MA, USA) according to the manufacturer's instructions. The qRT-PCR was performed with the PerfectStart® Green qPCR SuperMix (TransGen Biotech, Beijing, China) following the manufacturer's instructions. The primers were designed by Sangon Biotech (Shanghai, China) and the sequences were listed in Table 1. *β-actin* was used as an internal reference gene and the relative mRNA levels of the target genes were calculated by the $2^{-\Delta\Delta Ct}$ method.

Cell death analysis

Cell samples were washed three times with phosphate buffer saline (PBS) and stored at 4 °C. The apoptosis was detected using the TUNEL Apoptosis Detection Kit (KeyGENBioTECH, Nanjing, China) according to the manufacturer's instructions. $Tunel^+$ cells have stained green nuclei, and the DAPI-stained cells have blue nuclei. The $Tunel^+$ cells were counted and the numbers were statistically analyzed among groups.

Public data target prediction

The receptor data of the twelve TM4 cell lines were searched from NCBI (https://www.ncbi.nlm.nih.gov/geo/query/acc.cgi?acc=GSE142618). ChEMBL (https://www.ebi.ac.uk/chembl/), Swiss Target Prediction (http://swisstargetprediction.ch/), and Netlnfer (http://lmmd.ecust.edu.cn/netinfer/) were used to predict the targets for SchB.

Gene	Sequence
β-Actin	F: 5' -GTCAGGTCATCACTATCGGCAAT-3'
	R: 5'-AGAGGTCTTTACGGATGTCAACGT-3'
IL-6	F: 5'-AGCCACTGCCTTCCCTAC-3' R: 5'-TTGCCATTGCACAACTCTT-3'
IL-1β	F:5'-TGTGATGTTCCCATTAGAC-3' R: 5'-AATACCACTTGTTGGCTTA-3'
TNF-α	F: 5'- CCCCAAAGGGATGAGAAGTTC -3' R: 5'- CCTCCACTTGGTGGTTTGCT -3'
INOS	F: 5'-GAACTGTAGCACAGCACAGGAAAT-3' R: 5'-CGTACCGGATGAGCTGTGAAT-3'
COX-2	F: 5'-CGTACCGGATGAGCTGTGAAT-3' R: 5'-CCAGCACTTCACCCATCAGTT-3'
AR (Mouse)	F: 5'-CTGGGAAGGGTCTACCCAC-3'
	R: 5'-GGTGCTATGTTAGCGGCCTC-3'
AR(Human)	F: 5'-GTGCTGGACACGACAACAAC-3'
	R: 5'-GATCAGGGGCGAAGTAGAGC-3'
AR-V7 (Human)	F: 5'-AACAGAAGTACCTGTGCGCC-3'
	R: 5'-TCAGGGTCTGGTCATTTTGA-3'

Table 1. Sequences of the primers used for qRT-PCR.

Molecular docking

The 3D structure of AR (P10275) was obtained by using Alphaflod (https://alphafold.com/search/text/P10275). The structure files of SchB were downloaded from the Pubchem (https://pubchem.ncbi.nlm.nih.gov/, accessed July 26, 2023) database, and the molecular docking simulation was performed on the CBDOCK (https://cadd.labshare.cn/cb-dock/php/blinddock.php) website to generate structure files that can be used for docking.

Statistical analysis

The experiments were all carried out in triplicate. Data were presented as mean ± SEM and analyzed by GraphPad Prism7 (La Jolla, CA, USA). Differences between groups were analyzed by one way analysis of variance (ANOVA), and pairwise comparisons were performed by least-significant difference. $P < 0.05$ is considered statistically significant (* $P < 0.05$; ** $P < 0.01$).

Ethical statement

All the procedures were conducted according to the experimental practices and standards approved by the Animal Welfare and Research Ethics Committee at Jilin University.

Results

SchB ameliorates LPS-induced testicular inflammation

By using a mouse testicular inflammation model, the histopathological examination demonstrated that compared with the Con, Oil and SchB80 groups (Fig. 1A–C), the seminiferous epithelia in LPS group were badly destroyed, showing shrinked loose seminiferous epithelia, large areas of vacuolations, and sperm loss (Fig. 1D). However, the seminiferous epithelial structures in Sch_{40}LPS and Sch_{80}LPS groups (Fig. 1E,F) were maintained nearly normal similar with those in the Con, Oil, and SchB80 groups. Spermatogenesis was also observed and the vacuolation was significantly decreased in the seminiferous tubules of Sch_{40}LPS and Sch_{80}LPS groups (Fig. 1E,F). These observations were further confirmed by the quantifications of the sperm count and the average proportion of vacuolation area in each group (Fig. 1G,H).

SchB ameliorates LPS-induced BTB damage

Since Claudin-1 and ZO-1 are the main proteins of the BTB, next we performed immunofluorescent stainings of Claudin-1 and ZO-1on mouse testicular tissues. The results showed that compared with the Con, Oil and SchB80 groups (Fig. 2A–C), the expression of Claudin-1 in LPS group (Fig. 2D) was significantly decreased, while it's nearly restored to the control levels in Sch_{40}LPS and Sch_{80}LPS groups (Fig. 2E,F). The similar expression trends of ZO-1 were also observed in those tissues (Fig. 2G–L). The statistics of the fluorescence intensities of Claudin-1

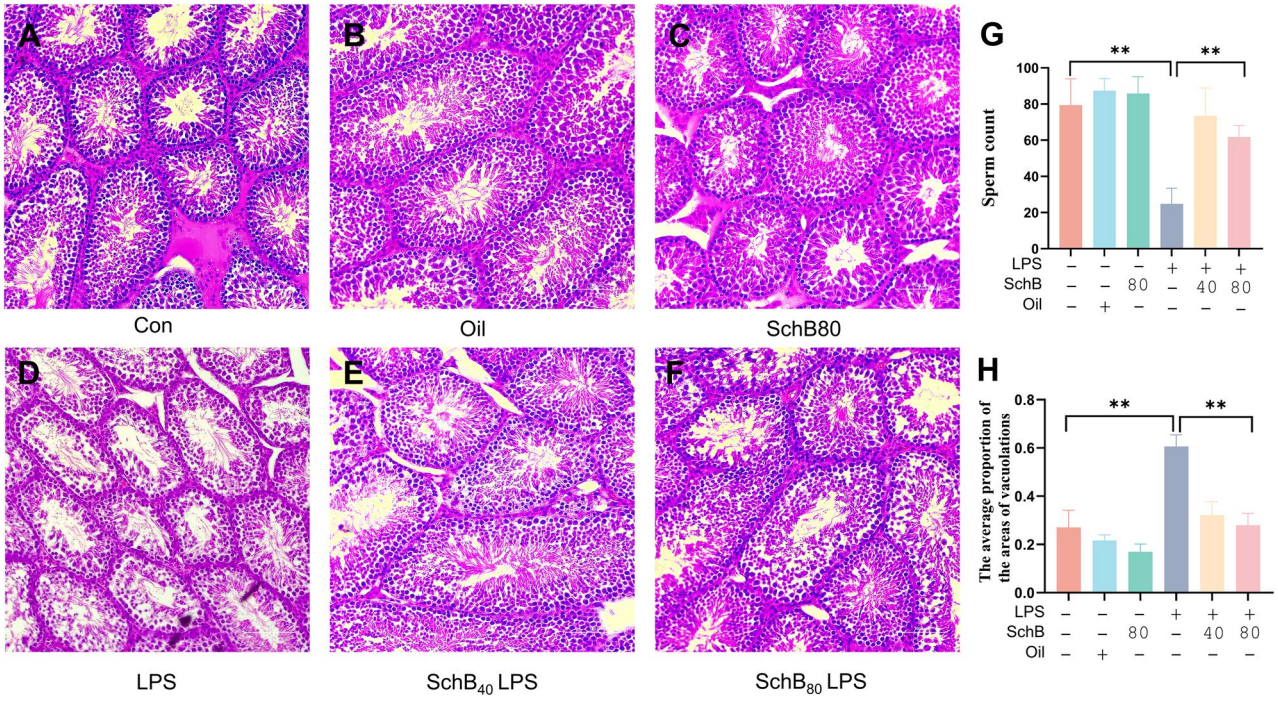

Figure 1. Schisandrin B (SchB) ameliorates LPS-induced mouse testicular inflammation. Mice were pretreated with SchB (40 mg/kg/d and 80 mg/kg/d respectively) for 72 h, following administration with 10 mg/kg LPS for 12 h. The testes were collected for hematoxylin–eosin (HE) staining. (**A**) Control (Con); (**B**) Olive oil control (Oil); (**C**) 80 mg/kg/d SchB (SchB80); (**D**) 10 mg/kg LPS (LPS); (**E**) 40 mg/kg/d SchB + LPS ($SchB_{40}$LPS); (**F**) 80 mg/kg/d SchB + LPS ($SchB_{80}$LPS); (**G**) The sperm count in each group; (**H**) The average proportion of vacuolation area in each group. **$P < 0.01$, Scale bar = 100 μm.

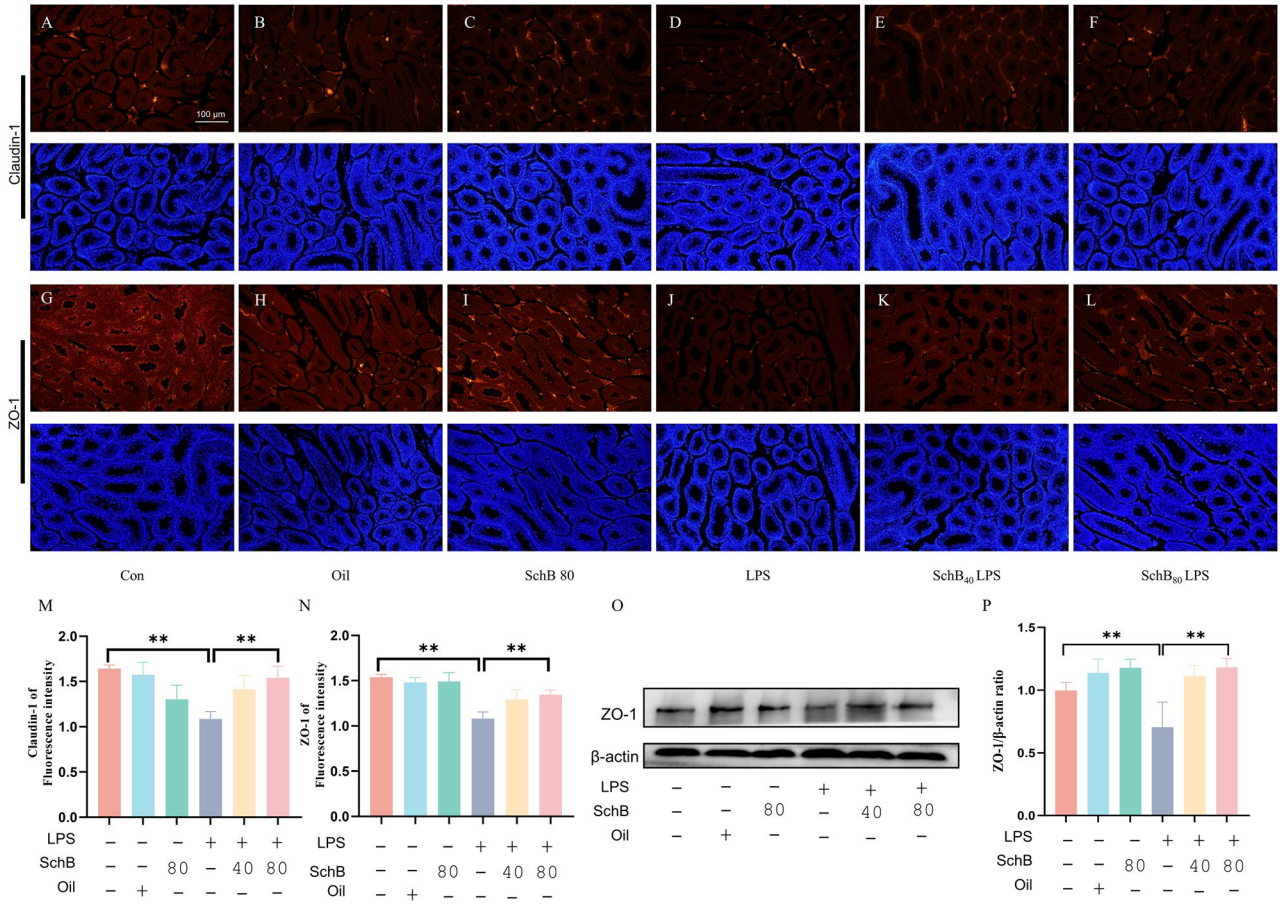

Figure 2. SchB ameliorates LPS-induced mouse BTB damage. Mice were pretreated as describe previously. The testicular sections were used for immunostaining. (**A**, **G**) Control (Con); (**B**, **H**) Olive oil control (Oil); (**C**, **I**) 80 mg/kg/d SchB (SchB80); (**D**, **J**) 10 mg/kg LPS (LPS); (**E**, **K**) 40 mg/kg/d SchB + LPS ($SchB_{40}$LPS); (**F**, **L**) 80 mg/kg/d SchB + LPS ($SchB_{80}$LPS); (**M**, **N**) Statistics of the fluorescent intensities of Claudin-1 and ZO-1 immunostainings, respectively. Red represents Claudin-1 and ZO-1 immunostaining, blue represents DAPI stained nuclei. (**O**) The protein levels of ZO-1 were determined by western blot; (**P**) Quantification and statistics for the corresponding protein band in (**O**). $^{**}P < 0.01$, Scale bar = 100 μm in (**A**–**L**).

and ZO-1 immunostainings (Fig. 2M,N) clearly confirmed these observations. Furthermore, ZO-1 was taken as the representative BTB molecule for western blot analysis, which showed the consistent results (Fig. 2O,P). These data imply that SchB can ameliorate LPS-induced mouse BTB damage.

SchB attenuates testicular inflammation

The qRT-PCR analysis showed that LPS stimulation remarkably increased the expression of inflammatory mediators including IL-6, IL-1β, TNF-α, COX-2 and iNOS, while SchB pretreatment dramatically decreased these changes, in mouse testes ($P < 0.01$, Fig. 3A–E). The protein expressions of COX-2 and iNOS were taken as the representative inflammatory mediators for further western blot analysis, which showed the similar changes (Fig. 3F–H).

SchB Inhibits LPS-induced inflammation in mSCs

To further evaluate the effects of SchB, LPS-induced mSCs were used as in vitro model. The cytotoxicity of SchB was determined by CCK-8 assay firstly, which showed that SchB pre-treatments at 5, 10, 15 and 20 μM didn't alter mSC viability with-/+ LPS stimulation, while SchB pretreatments at 30 and 40 μM decreased the cell viability significantly ($P < 0.01$, Fig. 4A). Accordingly, the lowest concentration (5 μM) was chosen for the following experiments. Subsequently, we assessed the anti-inflammatory effect of SchB in mSCs. The transcriptional analysis showed that LPS stimulation induced mRNA over-expressions of IL-6, IL-1β, TNF-α, COX-2, and iNOS, which were all dramatically reversed by SchB ($P < 0.01$, Fig. 4B–F). Consistently, LPS treatment elevated the protein levels of COX-2 and iNOS remarkably, while SchB decreased them markedly ($P < 0.01$, Fig. 4G–I).

NF-κB/MAPK signaling is involved in anti-inflammation of SchB

To elucidate the possible anti-inflammation mechanisms of SchB, several key molecules involved in the NF-κB (PP65/P65) and MAPK (P-JNK/JNK, PP38/P38, P-ERK/ERK) signaling pathways were analyzed by western blot

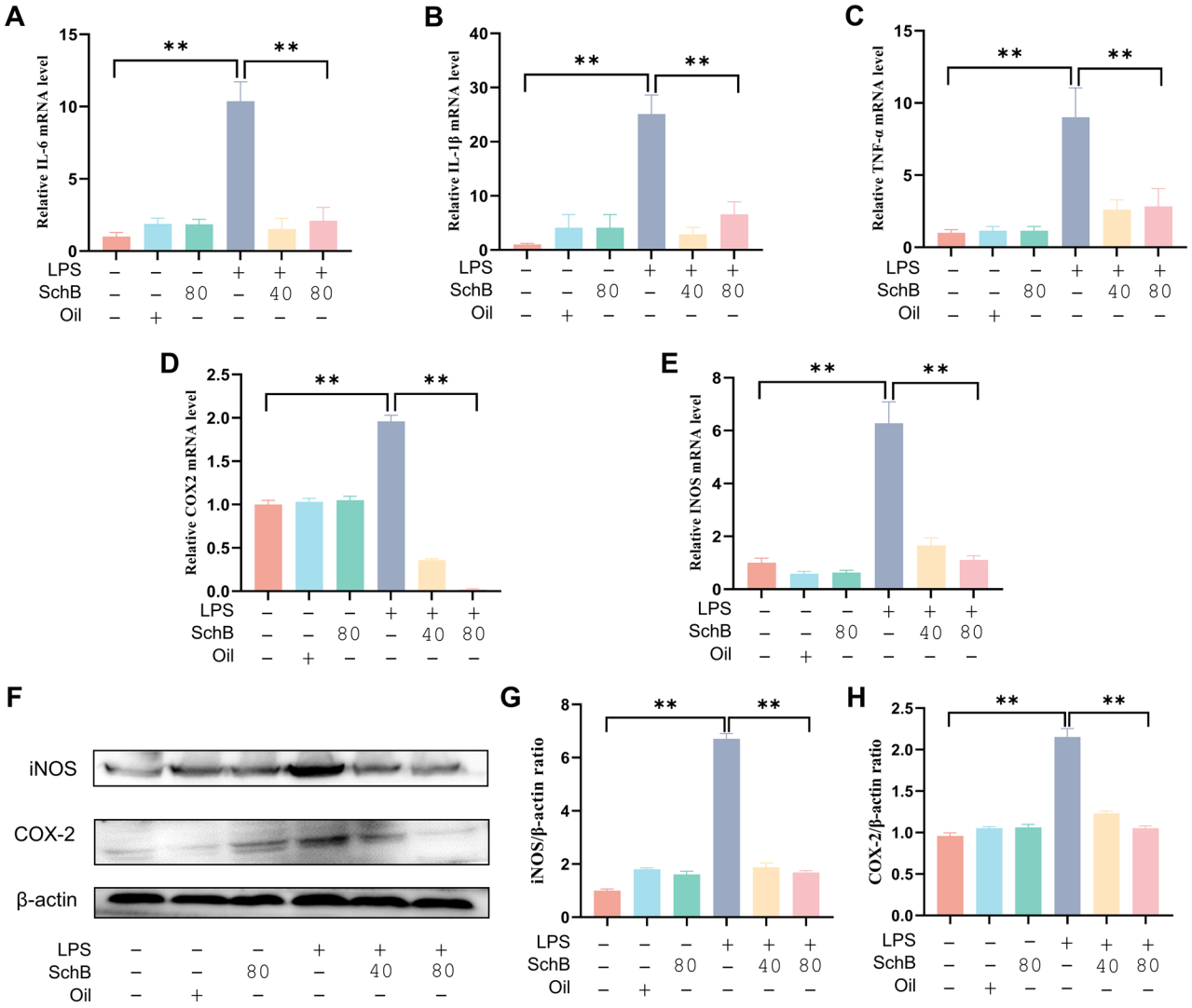

Figure 3. SchB attenuates the inflammation in mouse testes. Mice were pretreated similarly with Figs. 1–2. (**A**–**E**) Three testes from each group were used for RNA extraction. The mRNA levels of in-terleukin-6 (IL-6), interleukin-1β (IL-1β), tumor necrosis factor-α (TNF-α), cyclooxygenase 2 (COX-2) and induced nitric oxidesynthase (iNOS) were detected by quantitative real-time RT-PCR (qRT-PCR). (**F**) The protein levels of COX-2 and iNOS were determined by western blot. (G, H) Bar graphs represent quantitative results for the corresponding protein bands in (**F**). Values were expressed as mean ± SEM (n = 3). ** $P < 0.01$.

(Fig. 5A). The results showed that LPS increased the ratios of PP65/P65, P-JNK/JNK, PP38/P38 and P-ERK/ERK remarkably, while SchB decreased these ratios significantly ($P < 0.01$, Fig. 5A,B). These results suggest that the NF-κB/MAPK pathways are involved in the anti-inflammatory protection activity of SchB in LPS-stimulated mSC model.

SchB protects mSCs against LPS stimulation by inhibiting apoptosis

Inflammation usually leads to cell apoptosis. The effect of SchB on LPS-induced mSC apoptosis were examined by analyzing the expression of apoptosis-related proteins (Bax, Bcl2 and Pro-caspase-3). Compared with the control groups, the expressions of apoptotic marker Bax and Pro-caspase-3 were significantly increased, with decreased anti-apoptotic marker Bcl2, after LPS stimulation; however, they were all reversed by SchB treatment ($P < 0.01$, Fig. 6A,B). Consistently, Tunel staining revealed that there were significantly increased apoptotic mSCs in LPS group and remarkably decreased apoptotic cells in SchB treated group (Fig. 6C,D).

SchB inhibits mSC apoptosis by suppressing JNK activation

To further understand the molecular mechanism by which SchB inhibits mSC apoptosis, mSCs were incubated with JNK activator Anisomycin (5 μM) for one hour before SchB and LPS treatments. Similar changes of Bax, Bcl2 and Pro-caspase-3 as mentioned above were observed in mSCs treated free of Anisomyucin; whereas the apoptosis of mSCs was reactivated greatly after Anisomycin pretreatment ($P < 0.01$, Fig. 7A,B). Further tunel analysis showed that SchB decreased the number of Tunel$^+$ cells induced by LPS, while Anisomycin activation

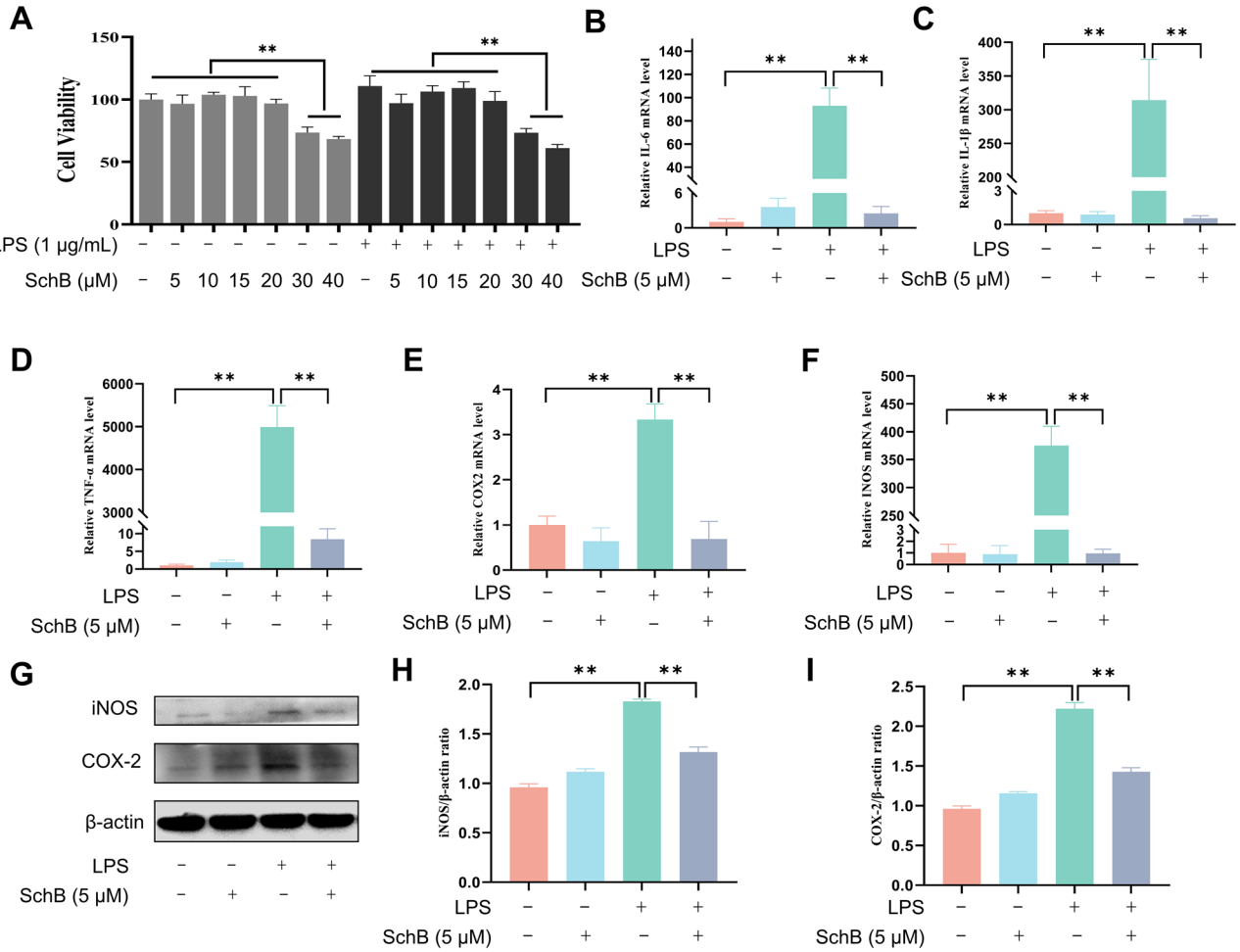

Figure 4. SchB inhibits LPS-induced inflammation in mSCs. (**A**) After serum starvation for 3 h, mouse Sertoli cells (mSCs) were administrated with SchB at different molar concentrations (5, 10, 15, 20, 30 and 40 μM) for 2 h, followed by treatment with LPS (1 μg/mL) for 12 h. Then, the cell viability was determined by Cell Counting Kit-8 (CCK-8). (**B**–**F**) The mSCs were administrated with SchB (5 μM) for 2 h, and next treated with LPS (1 μg/mL) for 12 h. Subsequently, the mRNA levels of IL-6, IL-1β, TNF-α, COX2 and iNOS were detected by qRT-PCR. (**G**) The protein levels of COX-2 and iNOS were determined by western blot. (**H**, **I**) Bar graphs represent quantitative results for the corresponding protein bands in (**G**). Values were expressed as mean ± SEM (n = 3). ** $P < 0.01$.

increased it again (Fig. 7C,D). These data together illustrate that the JNK signaling is involved in SchB inhibition of mSC apoptosis.

Androgen receptor (AR) is involved in SchB inhibition to mSC apoptosis

In order to further understand the molecular mechanism of SchB inhibition to mSC apoptosis, we performed bioinformatics analysis of 12 different mSC cell lines based on receptor prediction. Totally 420 receptors (supplement Table 1) were predicted and AR was targeted because it's shared among the three predictions (CheMBL, Swisstarget, and Netinfer, Fig. 8A,B). The molecular docking further showed that there is a SchB binding site in AR, implying SchB exerts its function by binding AR (Fig. 8C). The qRT-PCR results showed that LPS-induction upregulated AR expression, while SchB reversed the effects of LPS-stimulation. We further confirmed the regulation effects of SchB on AR and its variant AR-V7 using human macrophage cell line THP-1 under the same conditions (Fig. 9A). Subsequently, AR activator BSM-564929 (1 μM) was added before SchB treatment, and the expression of JNK signaling pathway-related proteins was detected by western blot (Fig. 9B). The results showed that BSM reversed the decrease in JNK expression caused by SchB, suggesting AR is involved in the regulation of JNK signals (Fig. 9C). In addition, BSM also reversed the expression of apoptosis-related proteins (Bax, Bcl2 and Pro-caspase-3, Fig. 9B,D-F). These data illustrate that SchB inhibit LPS-induced apoptosis by suppressing the AR-JNK pathway.

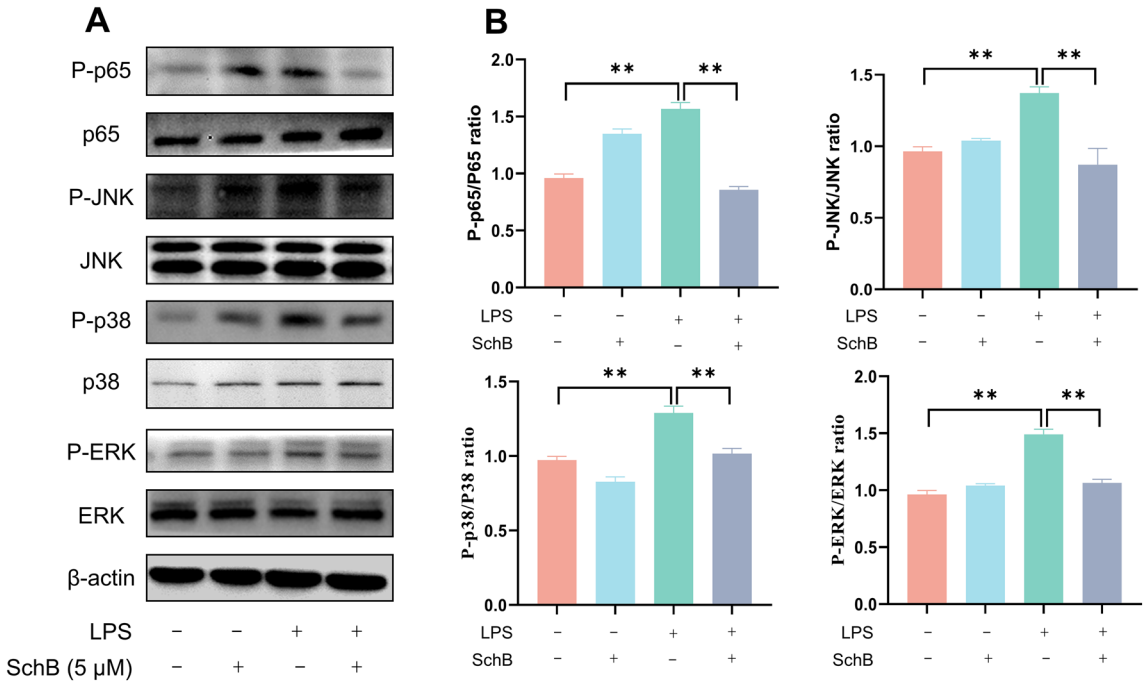

Figure 5. NF-κB and MAPK signaling pathways are involved in the anti-inflammatory effect of SchB in LPS-stimulated mSCs. (**A**) The mSCs were stimulated with SchB (5 μM) for 2 h, and then treated with LPS (1 μg/mL) for 12 h. The protein levels of NF-κB (PP65/P65) and MAPK (P-JNK/JNK, PP38/P38, P-ERK/ERK) pathways were determined by western blot. (**B**) Bar graphs represent quantitative results for the corresponding protein bands in (**A**).Values are presented as mean ± SEM (n = 3). ** $P < 0.01$.

Discussion

S. chinensis fruit is widely used as a dietary supplement, tonic and phytomedicine with a history of thousands of years in East Asia. Studies have demonstrated their effects on the central nervous system, liver, heart, lung, kidney and anticancer activity[13,15]. It's also used for improving male reproduction capability in traditional Chinese medicine[3,7,8]. However, its main components as well their effects on the seminiferous epithelium are unclear. SchB is one of the most important lignans of *S. chinensis* and the main effective compound of this herb. Elucidation of its effects on the testicular inflammation and testicular apoptosis might explain the pharmacological activity of *S. chinensis* on male reproduction, in view of testicular inflammation is one of the causes of male infertility. In this study, we found that SchB reduces the production of inflammatory rings by inhibiting the NF-κB and MAPK signaling pathways in mSC model, and inhibiting the LPS-induced inflammatory response in in vivo mouse model, thereby ameliorating LPS-induced mouse testicular inflammation. It also ameliorates LPS-induced mSC inflammation and apoptosis via the AR- JNK pathway.

Testicular inflammation is usually characterized by inflammatory cell infiltration and damage to the seminiferous tubules inside the testicles[20]. Peritoneal injection of LPS is the most frequently used protocol for mouse inflammation model. It induces testicular inflammation and stimulate the cells to produce large amounts of pro-inflammatory mediators such as IL-6, IL-1β, TNF-α, COX-2, and iNOS[21]. As the most important somatic cells in the seminiferous epithelium, SCs form the main structure of spermatogenic niche, the basal compartment (for spermatogonial stem cells, SSCs) and adluminal compartment (for differentiating germ cells), thus play pivotal functions including support, nurse/feeding, immunoregulation, protection, secretion, etc., in spermatogenesis. Therefore, we used mSCs as the model for in vitro experiments. In the present study, the in vivo experiment clearly indicates that LPS stimulation destroys the seminiferous epithelium and BTB, while SchB pretreatment protects it as nearly normal in controls, and the in vitro experiments indicate that SchB alleviates LPS-induced inflammation, i.e. reduces the expressions of inflammatory mediators like IL-6, IL-1β, TNF-α, COX-2, and iNOS. Recently, it's briefly reported that SchB repaired mouse spermatogenesis arrest and infertility without showing the related mechanisms[22]. Our data suggest that SchB improves male infertility by attenuating the testicular inflammation.

Studies have shown that LPS generally activates the NF-κB and MAPK signaling pathways[23,24]. Therefore, we next investigated the changes of the key molecules in these two pathways. Indeed, SchB downregulated the expressions of the key molecule PP65/P65 in NF-κB signaling pathway, and P-JNK/JNK, PP38/P38, P-ERK/ERK in MAPK pathway, implying they are involved in the protection of SchB against LPS-induced inflammation in the testes. SchB was reported to ameliorate inflammation in rat hind limb ischemia/reperfusion injury and mouse inflammatory bowel disease model[25,26]. It's also demonstrated that SchB could inhibit the activation of NF-κB signaling pathway caused by cigarette smoke[27]. Although its inhibition on NF-κB was documented, there is no detailed information involving mechanisms of SchB on the testicular tissues/cells available currently.

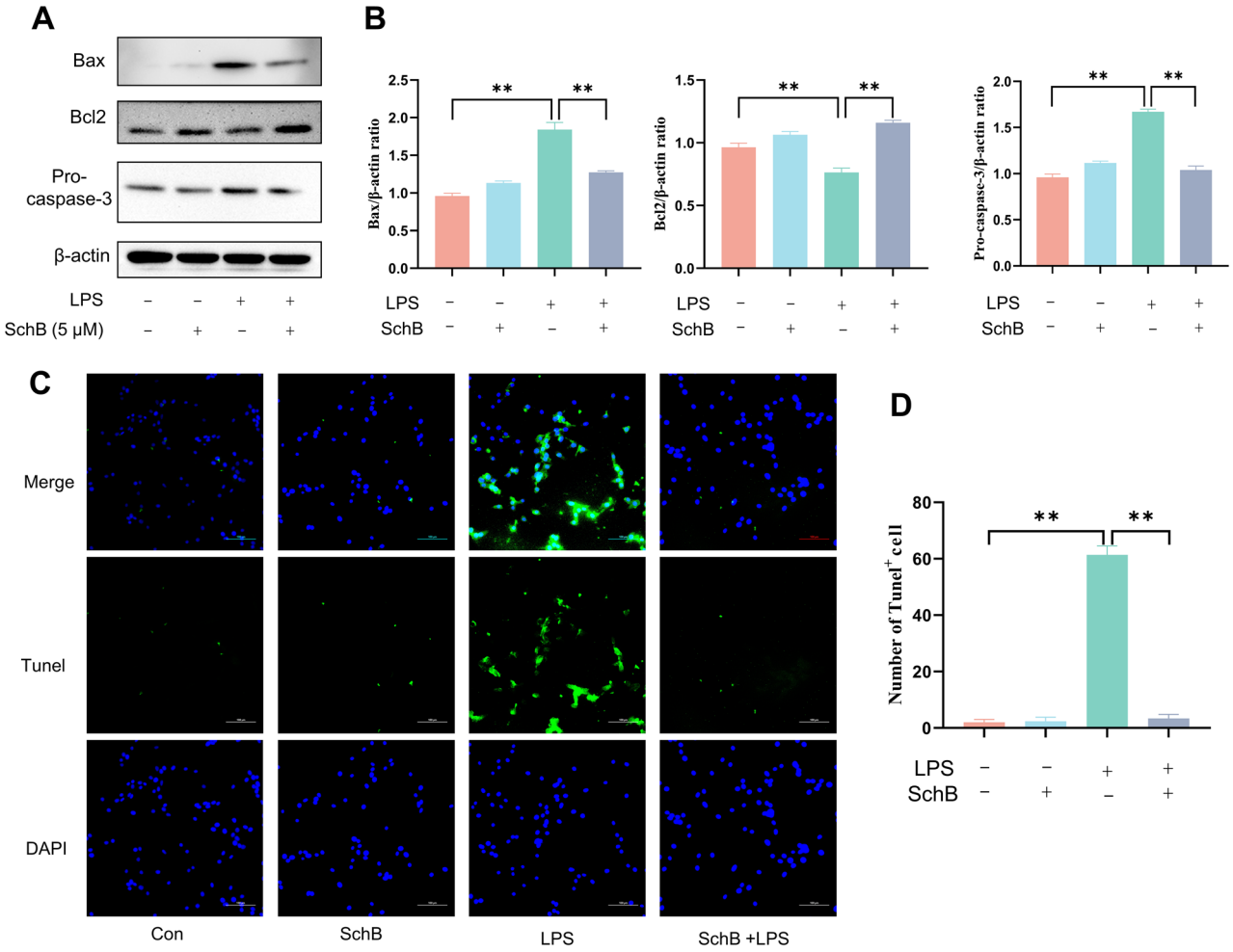

Figure 6. SchB protects mSCs by inhibiting LPS-induced apoptosis. (**A**) The mSCs were treated with 5 μM SchB for 2 h, then cultured with 1 μg/mL LPS for 12 h. The protein levels of apoptosis-related proteins (Bax, Bcl2 and Pro-caspase-3) were determined by western blot. (**B**) Bar graphs represent quantitative results for the corresponding protein bands in (**A**). (**C**) Tunel staining of mSCs, scale bar = 100 μm. The green cells represent the Tunel$^+$ cells. (**D**) Bar graph represents the number of Tunel$^+$ cells in (**C**). Values are presented as mean ± SEM (n = 3). ** $P < 0.01$.

Along with inflammation, apoptosis also occurs[28]. In this study, prominent apoptosis was observed in LPS stimulated mSCs by western blot and Tunel staining analysis. By contrast, the LPS-induced apoptosis in mSCs were sharply decreased by SchB pre-treatment. These data suggest that SchB is able to protect mSCs against apoptosis. Accumulated evidences showed that the activated JNKs and p38 MAPKs play key roles in balancing cell survival and death in response to both extracellular and intracellular stresses[29,30]. Our results together demonstrate that SchB play anti-apoptosis role in LPS-induced mSCs through JNK signaling pathway. To further uncover the molecular mechanism by which SchB inhibits mSC apoptosis, the cells were treated with JNK activator Anisomycin before SchB and LPS treatments. As expected, the expressions of apoptosis-related proteins inhibited by SchB were reactivated and the apoptotic mSCs re-increased markedly. Previous studies have shown that LPS elevated expressions of PARP[31], Caspase-7[32] and Caspase-9[33]. SchB might also function with these molecules to regulate apoptosis. Together, the above observations indicate that the JNK signaling is involved in SchB inhibition of mSC apoptosis. However, the detailed intrinsic and extrinsic mechanisms still need to be uncovered in future.

Subsequently, by the screening of bioinformatics database and molecular docking verification, as well the literature reviewing[34], we targeted the AR and illustrated that it might bind with SchB during its functioning. Indeed, AR expression was upregulated by LPS stimulation, while SchB treatment reversed this phenomenon; similarly, the expression of the JNK-related proteins and apoptotic-related protein were also reversed after AR activator treatment. AR pathway is necessary to complete spermatogenesis. It's able to regulate varied biological processes including proliferation, differentiation, apoptosis, inflammation, etc., in SCs as well as germ cells surrounded between SCs. Particularly, the regulation of AR signaling on testicular inflammation and apoptosis is closely related with the key molecule JNK in MAPK pathway[35]. It's well documented that JNK is an upstream signal for NF-κB[36]. Therefore, we consider that SchB mitigates LPS-induced inflammation and apoptosis by inhibiting the AR-JNK pathway.

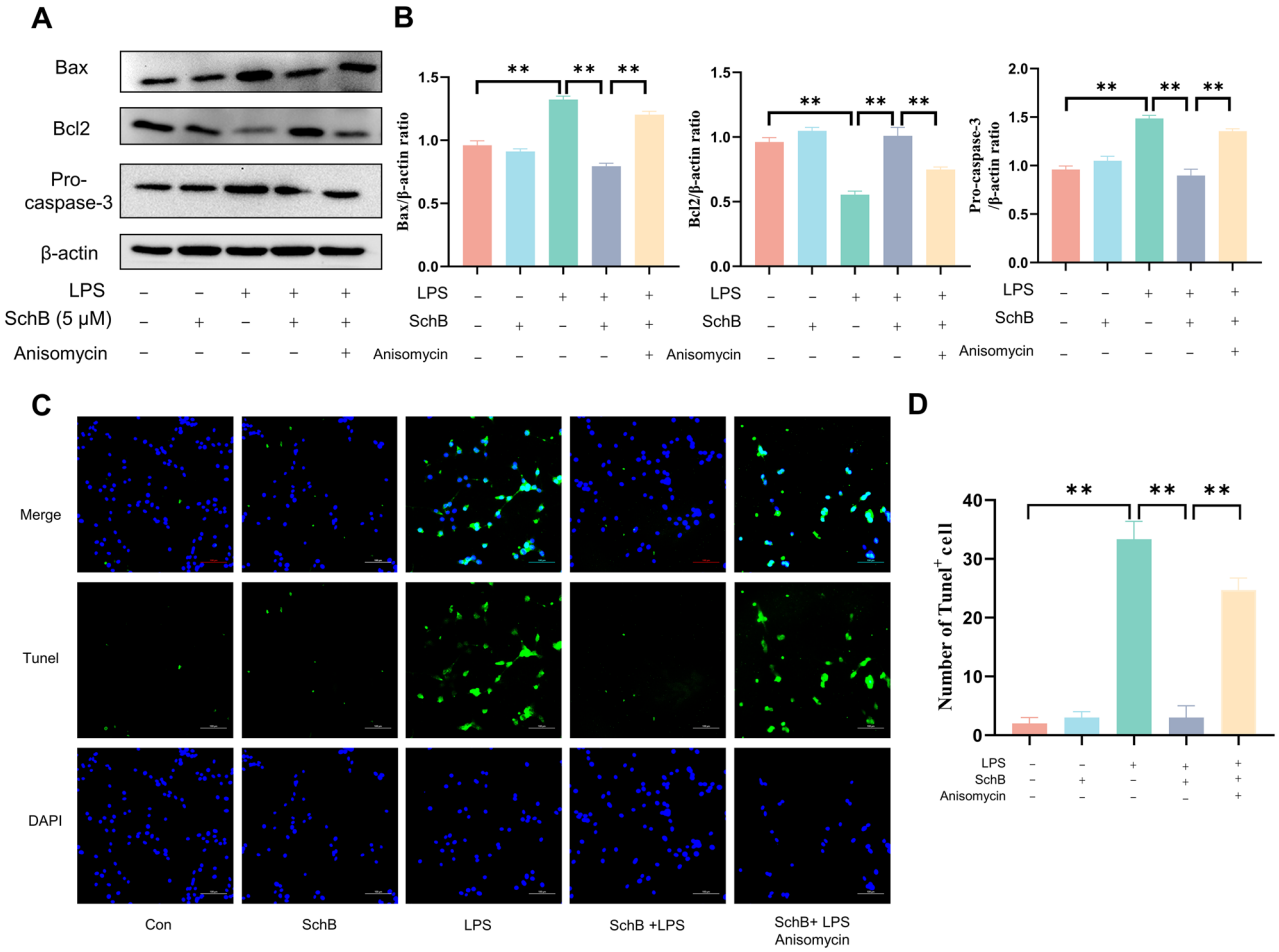

Figure 7. SchB inhibits LPS-induced apoptosis in mSCs by suppressing JNK activation. (**A**) The mSCs were pretreated with JNK activator Anisomycin (5 μM) for 1 h and then treated with SchB (5 μM) for 2 h, followed by exposure to LPS (1 μg/mL) for 12 h. The protein levels of Bax, Bcl2 and Pro-caspase-3 were determined by western blot. (**B**) Bar graphs represent quantitative results for the corresponding protein bands in (**A**). (**C**) Tunel staining of the treated mSCs, scale bar = 100 μm. The green cells represent the positive Tunel staining cells. (**D**) Bar graph represents the number of Tunel$^+$ cells in (**C**). Values are presented as mean ± SEM (n = 3). ** $P < 0.01$.

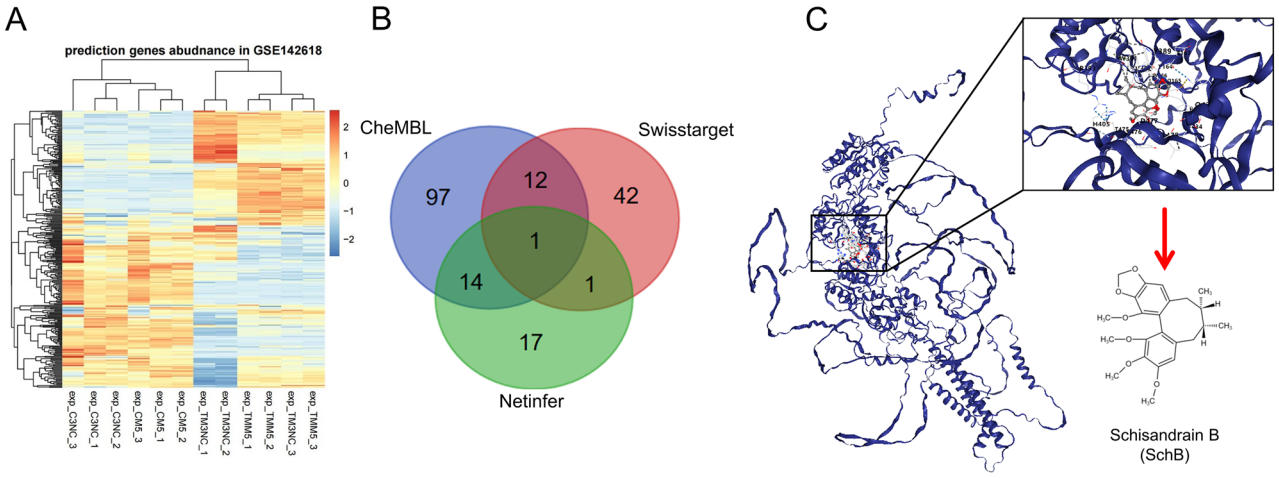

Figure 8. Receptor prediction and the molecular docking of AR. (**A**) Bioinformatics analysis of 12 different mSC lines based on receptor prediction; (**B**) Venn diagram of the three predictions; (**C**) AR and SchB molecular docking, showing there is a binding site for SchB in AR.

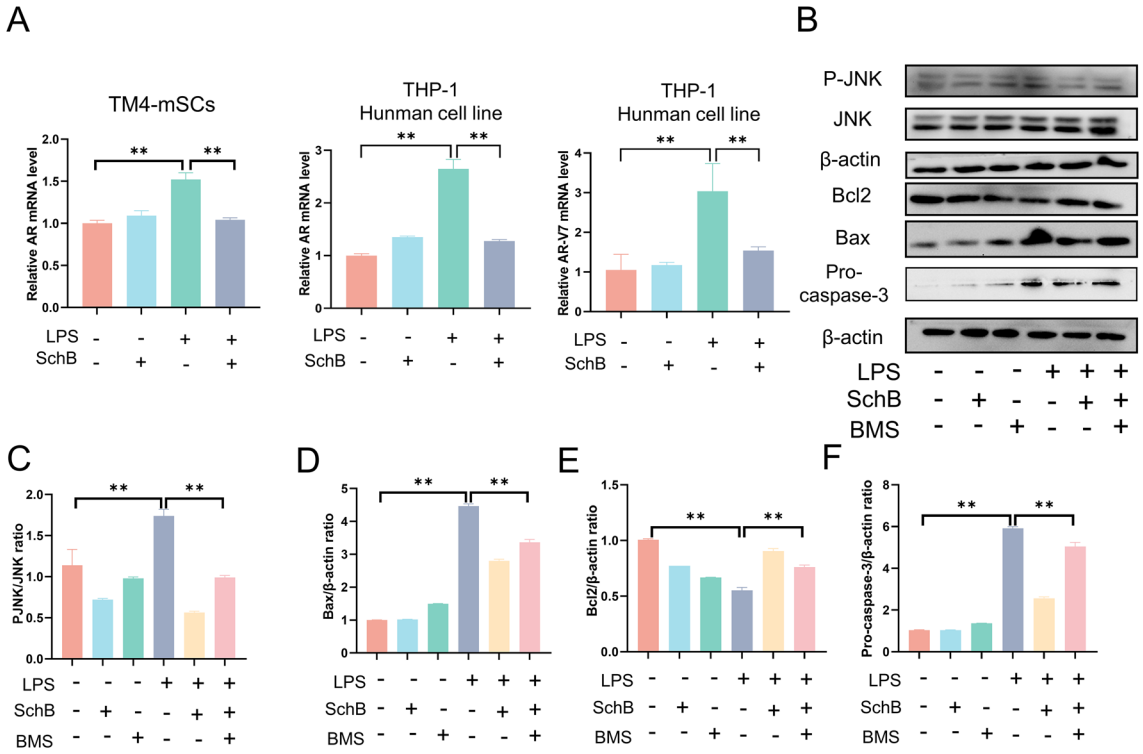

Figure 9. AR is involved in SchB inhibition to mSC apoptosis. (**A**) The mRNA levels of AR in TM4-mSCs and human cell line THP-1 were detected by qRT-PCR; mRNA of AR variant AR-V7 was also detected in THP-1. (**B**) The mSCs were pretreated with AR activator BMS-564929 (1 μM) for 1 h and then treated with SchB (5 μM) for 2 h, followed by exposure to LPS (1 μg/mL) for 12 h. The protein levels of JNK, P-JNK, Bax, Bcl2, and Caspase-3 were determined by western blot. (C-F) Bar graphs represent quantitative results for the corresponding protein bands in (B). ** $P < 0.01$.

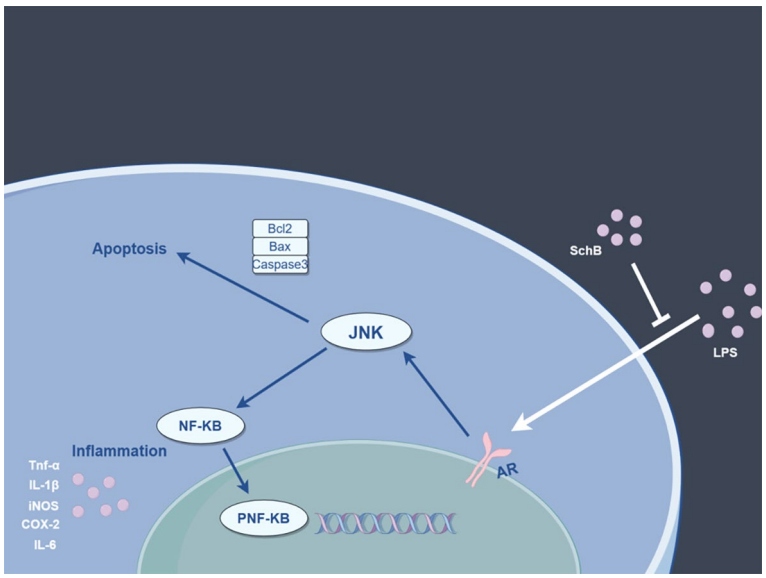

Figure 10. Diagram of SchB ameliorates mouse testicular inflammation and apoptosis via AR-JNK pathway. LPS induces testicular inflammation and apoptosis, while SchB attenuates the inflammatory response and apoptosis through AR-JNK signaling pathway.

To summarize, the present study used LPS-induced mouse testicular inflammation and mSC inflammation as the in vivo and in vitro models to explore the effects and mechanisms of SchB on the testicular inflammation and apoptosis. We found that SchB ameliorates the damage and reduces the production of pro-inflammatory mediators in the testicular tissues. Similarly, SchB also attenuates LPS-induced apoptosis and inflammation in mSCs by inhibiting the AR-JNK pathway (Fig. 10). Collectively, SchB exerts a protective activity against testicular inflammation and apoptosis. These findings are helpful to explain the pharmacological activities of the herbal medicine *S. chinensis* on male reproduction.

Data availability

The data that support the findings of this study are available from the corresponding author, upon reasonable request.

Received: 7 February 2024; Accepted: 5 August 2024
Published online: 08 August 2024

References

1. Levine, H. *et al.* Temporal trends in sperm count: a systematic review and meta-regression analysis. *Hum. Reprod. Update* **23**, 646–659 (2017).
2. Schuppe, H. C. *et al.* Chronic orchitis: a neglected cause of male infertility?. *Andrologia* **40**, 84–91 (2008).
3. Feng, R. *et al.* The ameliorative effect of melatonin on LPS-induced Sertoli cells inflammatory and tight junctions damage via suppression of the TLR4/MyD88/NF-κB signaling pathway in newborn calf. *Theriogenology* **179**, 103–116 (2022).
4. Zhu, C. L. *et al.* Antimicrobial peptide MPX attenuates LPS-induced inflammatory response and blood-testis barrier dysfunction in Sertoli cells. *Theriogenology* **189**, 301–312 (2022).
5. Yang, K. *et al.* A comprehensive review of ethnopharmacology, phytochemistry, pharmacology, and pharmacokinetics of Schisandra chinensis (Turcz.) Baill. and Schisandra sphenanthera Rehd. et. Wils.. *J. Ethnopharmacol.* **284**, 114759 (2022).
6. Kang, D. *et al.* Systematically identifying the hepatoprotective ingredients of schisandra lignan extract from pharmacokinetic and pharmacodynamic perspectives. *Phytomedicine* **53**, 182–192 (2019).
7. Szopa, A., Ekiert, R. & Ekiert, H. Current knowledge of Schisandra chinensis (Turcz.) Baill. (Chinese magnolia vine) as a medicinal plant species: a review on the bioactive components, pharmacological properties, analytical and biotechnological studies. *Phytochem. Rev.* **16**, 195–218 (2017).
8. Zhu, P., Li, J., Fu, X. & Yu, Z. Schisandra fruits for the management of drug-induced liver injury in China: A review. *Phytomedicine* **59**, 152760 (2019).
9. Nasser, M. I. *et al.* A comprehensive review on Schisandrin B and its biological properties. *Oxid. Med. Cell. Longev.* **2020**, 2172740 (2020).
10. Leong, P. K. & Ko, K. M. Schisandrin B: A double-edged sword in nonalcoholic fatty liver disease. *Oxid. Med. Cell. Longev.* **2016**, 6171658 (2016).
11. Jiang, E. P. *et al.* Schisandrin B protects PC12 cells against oxidative stress of neurodegenerative diseases. *Neuroreport* **26**, 360–366 (2015).
12. Leong, P. K., Chen, N. & Ko, K. M. Mitochondrial decay in ageing: 'Qi-invigorating' schisandrin B as a hormetic agent for mitigating age-related diseases. *Clin. Exp. Pharmacol. Physiol.* **39**, 256–264 (2012).
13. Sun, Y. X. *et al.* Schisandrin A and B affect subventricular zone neurogenesis in mouse. *Eur .J. Pharmacol.* **740**, 552–559 (2014).
14. Cai, N. N. *et al.* Schisandrin A and B enhance the dentate gyrus neurogenesis in mouse hippocampus. *J. Chem. Neuroanat.* **105**, 101751 (2020).
15. Cai, N. N. *et al.* Schisandrin A and B affect the proliferation and differentiation of neural stem cells. *J. Chem. Neuroanat.* **119**, 102058 (2022).
16. Zhang, M., Xu, L. & Yang, H. Schisandra chinensis fructus and its active ingredients as promising resources for the treatment of neurological Diseases. *Int. J. Mol. Sci.* **19**, 1970 (2018).
17. Qin, J. H., Lin, J. R., Ding, W. F. & Wu, W. H. Schisandrin B improves the renal function of IgA nephropathy rats through inhibition of the NF-κB signalling pathway. *Inflammation* **42**, 884–894 (2019).
18. Griswold, M. D. 50 years of spermatogenesis: Sertoli cells and their interactions with germ cells. *Biol. Reprod.* **99**, 87–100 (2018).
19. Meroni, S. B. *et al.* Molecular mechanisms and signaling pathways involved in Sertoli Cell proliferation. *Front. Endocrinol.* **10**, 224 (2019).
20. Jungwirth, A. *et al.* European Association of Urology guidelines on Male Infertility: The 2012 update. *Eur. Urol.* **62**, 324–332 (2012).
21. Ok, F., Kaplan, H. M., Kizilgok, B. & Demir, E. Protective effect of Alpha-linolenic acid on lipopolysaccharide-induced orchitis in mice. *Andrologia* **52**, e13667 (2020).
22. Zou, D. X. *et al.* Schisandrin B for the treatment of male infertility. *Clin. Transl. Med.* **11**, e333 (2021).
23. Zusso, M. *et al.* Ciprofloxacin and levofloxacin attenuate microglia inflammatory response via TLR4/NF-kB pathway. *J. Neuroinflamm.* **16**, 148 (2019).
24. Dong, N. *et al.* Astragalus polysaccharides alleviates LPS-induced inflammation via the NF-κB/MAPK signaling pathway. *J. Cell. Physiol.* **235**, 5525–5540 (2020).
25. Zhu, N. *et al.* Schisandrin B Prevents hind limb from ischemia-reperfusion-induced oxidative stress and inflammation via MAPK/NF-κB pathways in rats. *Biomed. Res. Int.* **2017**, 4237973 (2017).
26. Liu, W. *et al.* Suppression of MAPK and NF-κ B pathways by schisandrin B contributes to attenuation of DSS-induced mice model of inflammatory bowel disease. *Pharmazie* **70**, 598–603 (2015).
27. Jia, R. *et al.* Protective effects of Schisandrin B on cigarette smoke-induced airway injury in mice through Nrf2 pathway. *Int. Immunopharmacol.* **53**, 11–16 (2017).
28. Li, L., Wan, G., Han, B. & Zhang, Z. Echinacoside alleviated LPS-induced cell apoptosis and inflammation in rat intestine epithelial cells by inhibiting the mTOR/STAT3 pathway. *Biomed. Pharmacother.* **104**, 622–628 (2018).
29. Wagner, E. F. & Nebreda, A. R. Signal integration by JNK and p38 MAPK pathways in cancer development. *Nat. Rev. Cancer* **9**, 537–549 (2009).
30. Yue, J. & López, J. M. Understanding MAPK Signaling pathways in apoptosis. *Int. J. Mol. Sci.* **21**, 2346 (2020).
31. Sriram, C. S., Jangra, A., Gurjar, S. S., Mohan, P. & Bezbaruah, B. K. Edaravone abrogates LPS-induced behavioral anomalies, neuroinflammation and PARP-1. *Physiol. Behav.* **154**, 135–144 (2016).
32. Eslami, M., Alizadeh, L., Morteza-Zadeh, P. & Sayyah, M. The effect of Lipopolysaccharide (LPS) pretreatment on hippocampal apoptosis in traumatic rats. *Neurol. Res.* **42**, 91–98 (2020).
33. Li, L., Wang, H. H., Nie, X. T., Jiang, W. R. & Zhang, Y. S. Sodium butyrate ameliorates lipopolysaccharide-induced cow mammary epithelial cells from oxidative stress damage and apoptosis. *J. Cell. Biochem.* **120**, 2370–2381 (2019).

34. Tang, X. *et al.* Posttreatment with dexmedetomidine aggravates LPS-induced myocardial dysfunction partly via activating cardiac endothelial α2A-AR in mice. *Int. Immunopharmacol.* **116**, 109724 (2023).
35. Wang, J. M., Li, Z. F. & Yang, W. X. What does androgen receptor signaling pathway in Sertoli cells during normal spermatogenesis tell us?. *Front. Endocrinol.* **13**, 838858 (2022).
36. Bai, Y. *et al.* Isoliquiritigenin inhibits microglia-mediated neuroinflammation in models of Parkinson's disease via JNK/AKT/NFκB signaling pathway. *Phytother. Res.* **37**, 848–859 (2023).

Acknowledgements

This work was financially supported by the National Natural Science Foundation of China (Grant No.32172803 and 31872434).

Author contributions

Bo-Yang Zhang: Writing – original draft, Methodology, Investigation, Data curation, Visualization. Rui Yang: Methodology, Validation, Data curation, Resources, Writing – original draft. Wen-Qian Zhu: Methodology, Resources, Formal analysis. Chun-Ling Zhu: Validation, Investigation, Formal analysis. Lan-Xin Chen: Validation, Investigation, resources. Yan-Sen Zhao, Yan Zhang, Yue-Qi Wang and Dao-Zhen Jiang: Validation, Investigation. Bo Tang: Writing – review & editing, Supervision. Xue-Ming Zhang: Conceptualization, Supervision, Project administration, Funding acquisition.

Competing interests

The authors declare no competing interests.

Additional information

Supplementary Information The online version contains supplementary material available at https://doi.org/10.1038/s41598-024-69389-1.

Correspondence and requests for materials should be addressed to X.-M.Z.